

Imaging with $\tau = 0$ versus $t = 0$: towards including headwaves into imaging and internal multiple attenuation theory

Bogdan G. Nita and Arthur B. Weglein

Abstract

The internal multiples attenuation algorithm derived from inverse scattering series techniques can be interpreted as a sequence of un-collapsed migrations with the reference medium velocity and restricted to lower-higher-lower pseudo-depths (Weglein et al. 1997, Weglein et al. 2003). The arrivals in the data are regarded as sub-events in the creation of a multiple. These sub-events are imaged through these migrations with $t = 0$ imaging condition. In this paper we discuss both the $t = 0$ and the $\tau = 0$ imaging condition and show that the latter is more general in its ability to image, in addition, events that exhibit a horizontal propagation part in their path (e.g. headwaves along a horizontal interface). This research is part of our strategy to include more of the returning signal, information bearing or not, in our analysis and processing.

1 Introduction

The inverse scattering series is a multi-dimensional inversion procedure that directly determines physical properties using only recorded data and a reference medium. This inversion process can be thought of as performing the following four tasks: (1) free surface multiple removal, (2) internal multiple removal, (3) location of reflectors in space and (4) identification of medium property changes across reflectors. These tasks were associated with subseries of the full series, subseries which, if identified, would perform their job as if no other task existed in the series. Two immediate advantages of this separation of tasks are the favorable convergence properties of the subseries and the ability to judge the effectiveness of each step before proceeding on to the next. Since the entire process requires only data and reference medium information, it is reasonable to assume that intermediate steps that are associated with achieving that objective would also be attainable with only the reference medium and data.

Subseries that exhibit this property have been identified for all four tasks (Weglein et al. 2003 and references therein). Algorithms resulting from the subseries for the task of free surface and internal multiple attenuation have been successfully applied to field data (Weglein et al. 2003). The internal multiples attenuation algorithm derived from inverse scattering series techniques can be interpreted as a sequence of un-collapsed migrations with the reference

medium velocity and restricted to lower-higher-lower pseudo-depths (Weglein et al. 1997, Weglein et al. 2003). The arrivals in the data are regarded as sub-events in the creation of a multiple. The sub-events are imaged through these migrations with $t = 0$ imaging condition. In this paper we discuss the $t = 0$ versus the $\tau = 0$ imaging condition and show that the latter is more general in its ability to image, in addition, events that exhibit a horizontal propagation part in their path, e.g. headwaves along a horizontal interface and reflections from dipping reflectors. The purpose of this research is to expand our understanding of the events and sub-events in the returning signal and it is part of our strategy to include more of this signal, information bearing or not, in our analysis and processing.

The idea of using $\tau = 0$ as an imaging condition has been used by Clayton and McMechan (1981) to image refraction data to produce velocity-depth profiles from recorded data. Their method involves a slant-stack of the data to produce a wavefield in the $p - \tau$ domain, where p is the horizontal slowness, and a downward continuation and imaging with $\tau = 0$.

The plan for this paper is as follows. In Section 2 we give a brief description of the internal multiples attenuation algorithm derived from the inverse scattering series techniques. In Section 3 we present headwaves as prime events or sub-events of composite events using both ray and wave front diagrams; in Section 4, we briefly discuss the pre-stack constant velocity phase-shift migration. Section 5 presents a comparison between the travel time t and the vertical time τ . In Section 6 we present an analytic example of imaging headwaves from horizontal interfaces using $\tau = 0$ imaging condition. Some conclusions are drawn in Section 7. Throughout the paper, "horizontal" refers to the direction parallel to the measurement surface in a 3D seismic experiment.

2 Internal multiples attenuation algorithm

The second term in the inverse scattering subseries for internal multiple attenuation is (see e.g. Weglein et al 2003)

$$\begin{aligned}
 b_3(k_g, k_s, q_g + q_s) &= \frac{1}{(2\pi)^2} \int \int dk_1 e^{-iq_1(\epsilon_g - \epsilon_s)} dk_2 e^{iq_2(\epsilon_g - \epsilon_s)} \\
 &\times \int_{-\infty}^{\infty} dz_1 e^{i(q_g + q_1)z_1} b_1(k_g, k_1, z_1) \int_{-\infty}^{z_1} dz_2 e^{i(-q_1 - q_2)z_2} b_1(k_1, k_2, z_2) \\
 &\times \int_{z_2}^{\infty} dz_3 e^{i(q_2 + q_s)z_3} b_1(k_2, k_s, z_3)
 \end{aligned} \tag{1}$$

where $z_1 > z_2$ and $z_2 > z_3$ and b_1 is defined in terms of the original pre-stack data with free surface multiples eliminated, D' , to be

$$D'(k_g, k_s, \omega) = (-2iq_s)^{-1} B(\omega) b_1(k_g, k_s, q_g + q_s) \tag{2}$$

with $B(\omega)$ being the source signature.

The terms $b_1(k_g, k_s, z)$ in formula (1) can be thought of as being obtained through the following procedure. Start with the effective data in the $f - k$ domain, $b_1(k_g, k_s, \omega)$, and downward continue the source and receiver by applying a phase-shift $e^{ik_z z} b_1(k_g, k_s, \omega)$. Subsequent integration over k_z to obtain $b_1(k_g, k_s, z)$ is a simple Jacobian away from integration over ω ($t = 0$ imaging condition). The algorithm can hence be interpreted as a sequence of un-collapsed migrations restricted to lower-higher-lower pseudo-depths. Notice that any arrival in the data is regarded as a sub-event by the algorithm and imaged through the process above. Three prime events in the data will create, and hence attenuate, a first order multiple; subsequent composite arrivals will create and attenuate higher order multiples.

The presence of an implicit $t = 0$ imaging condition in the algorithm motivates its comparison against imaging with $\tau = 0$, where τ is the vertical time. We found the latter to be more general in its ability to collapse any horizontal propagations and hence to image properly, in addition, events which contain horizontal parts in their propagation paths, e.g. headwaves along horizontal interfaces. To be able to image a larger class of events (or sub-events) using a different imaging condition means to be able to attenuate a larger class of internal multiples and reduce the number of artifacts in the de-multipled data.

Although the rest of the paper mainly discusses headwaves due to horizontal interfaces we mention that the results apply to all prime events or sub-events of composite events which contain horizontally propagating parts.

3 Headwaves as prime events or sub-events of composite events

The propagation path of the headwaves (see Figure 1), also known in the literature as conical or lateral waves, was first recognized by Mohorovicic during his studies of the arrival time of certain waves from an earthquake in 1909. The headwave has a linear relationship between arrival time and horizontal range and, at sufficient offset, it is the first arriving wave (attribute which accounts for its name). The one who originated the theory of headwaves as recognizably distinct arrivals was Jeffreys (1926) although the source/medium geometries needed for such a wave to develop have been known since 1904 and referred under the general term "Lamb's Problem". An excellent brief history of the headwaves can be found in Cerveny and Ravindra (1971).

A simple picture of the headwave can be given using the Huygens Principle which was first applied to these problems by Merten (1927) and is described in many books on seismology or wave propagation. The simplest case, in which the physical conditions for headwaves to occur are satisfied, is that of two semi-infinite homogeneous liquid media. We assume that the point source is located at s at a distance z_1 from a horizontal interface separating two

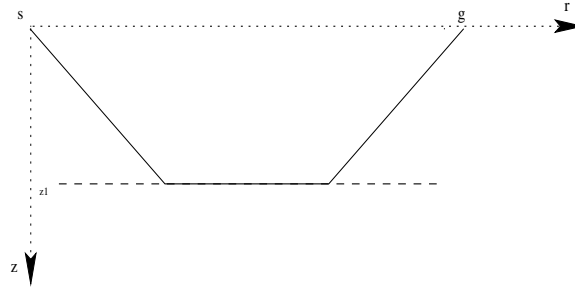


Figure 1: A ray picture of the headwave.

media such that the velocity of propagation in the second medium, c_1 , is higher than the velocity of propagation in the first medium, c_0 (see Figure 2).

The cylindrical coordinates of an arbitrary point are (r, z, φ) where r is the distance from the vertical axis in a horizontal plane. We will consider only the two dimensional section (r, z) with $\varphi = const$. Assume that the source starts to emit waves at time $t = 0$. For $t < z_1/c_0$, i.e. before the wave reaches the interface, only the incident wave exists (see Figure 2a). In this picture, the point C indicates the critical incidence. The wavefront is a sphere with the center at s and radius $R = \sqrt{r^2 + (z - z_1)^2}$ proportional to t (i.e. $t = R/c_0$). For $t = z_1/c_0$, the wavefront of the incident wave reaches the interface and it is tangent to it. As t increases further, reflected and refracted waves appear, as each point on the interface hit by the incidence wave becomes a source of disturbance according to Huygens principle. The wave fronts of these waves for $z_1/c_0 < t < z_1/(c_0 \cos i_c)$ are shown in Figure 2b. The wave fronts of the incident, reflected and transmitted waves are connected at the point P on the interface which moves along the interface with increasing time. The speed of the point P along the interface can be calculated to be

$$c_P = \frac{c_0}{\sin i_P} \tag{3}$$

where i_P is the angle between the ray incident at the point P and the vertical. The angle i_P increases with horizontal distance r , and so does $\sin i_P$ which means that the velocity of

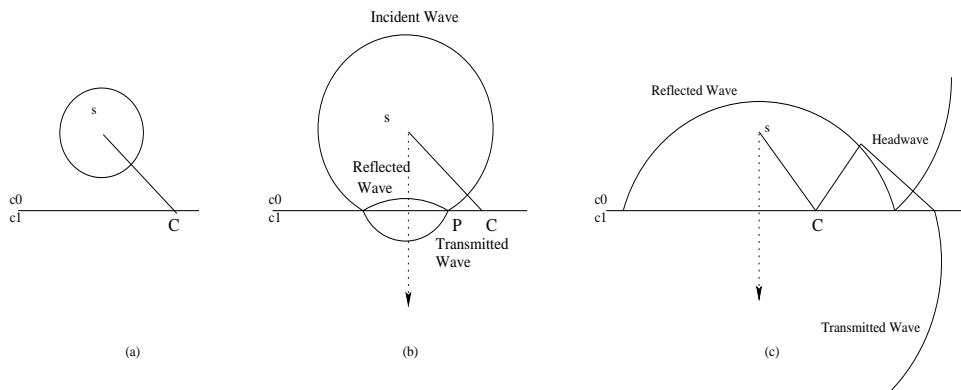


Figure 2: Wavefront diagrams showing the development of the headwave.

the point P along the interface, c_P , decreases. While $c_P > c_1$ the situation remains the same with all three wavefronts connected at the point P . However, for $t = z_1 / (c_0 \cos i_c)$, where $i_c = \sin^{-1}(c_0/c_1)$, the point P reaches the point C where we have

$$c_P = \frac{c_0}{\sin i_c} = c_1. \quad (4)$$

For larger t , we have $c_P < c_1$ and the transmitted wave, propagating from the point C in the second medium will be more advanced than the incident and reflected waves (see Figure ??c). Points on the interface which are reached by the refracted wave first, i.e. all the points with r coordinate bigger than the r coordinate of the point C , will become centers of disturbances propagating back into the first medium with velocity c_0 . These disturbances form the headwave, the envelop of these propagations being its wave front. As the velocities c_0 and c_1 are constant, the wavefront of the headwave is a straight line (in three dimensions it is the frustum of a cone).

An important feature that emerges from the wavefront diagram representation outlined above is that the headwaves are due to the curvature of the wavefront and hence it would be impossible to create headwaves if the wave impinging on the interface would be a plane-wave. This, and the fact that the headwave itself is a plane-wave, leads to the conclusion that a headwave cannot create a multiple of itself and hence the seismic event pictured in Figure 3 is not a real one.

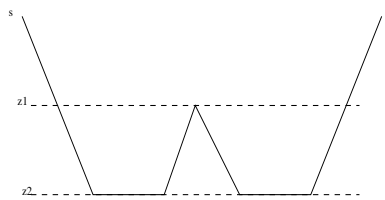
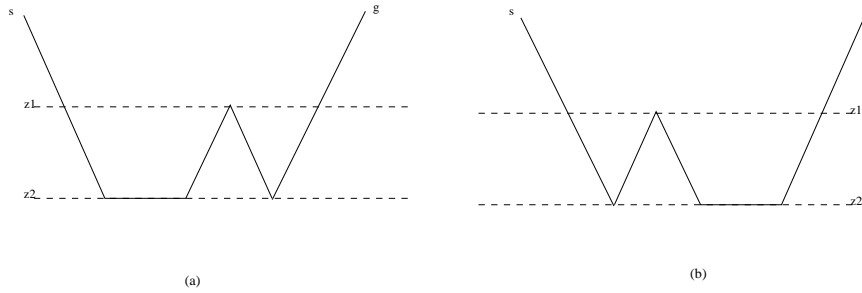


Figure 3: *An impossible event in which headwaves are sub-events.*

However, headwaves can occur as sub-events in a composite event if for example the other sub-events are regular reflections; we call these kind of events, i.e. containing a headwave as a sub-event, refracted multiples. The refracted multiples can be divided into free-surface and internal refracted multiples depending whether any downward reflection takes place at the free-surface, or they all take place inside the actual medium (Figure 4 shows examples of first order internal refracted multiples).

The free surface refracted multiples are presently removed by free-surface de-multiple algorithms (Dragoset (2003)). In this paper we show that, while the $t = 0$ imaging condition is not physically appropriate to handle events containing horizontally propagating parts (e.g. headwaves from horizontal reflectors), the $\tau = 0$ imaging condition has the ability to image them at the correct depth. An analytic example showing this is given in Section 6.

Figure 4: *First order internal refracted multiples.*

4 Pre-stack constant velocity phase-shift migration

In this section we give a brief mathematical account of the pre-stack constant velocity phase-shift migration following Stolt and Benson (1986).

The data $D(x_g, y_g | x_s, y_s; t)$ recorded on the measurement surface is the expression of an up-going wavefield P calculated at $z = 0$, i.e.

$$D(x_g, y_g | x_s, y_s; t) = P(x_g, y_g, 0 | x_s, y_s, 0; t). \quad (5)$$

In this equation t represents the travel-time of the wave, i.e. the time it takes for the signal to travel from the source to the reflector and back to the receiver. The amplitude of the returning signal is a function which depends on the reflectivity $M(x, y, z)$ where (x, y, z) denotes a point on the reflector. Migration is the operation of mapping the data D onto the reflectivity M

$$D(x_g, y_g | x_s, y_s; t) \rightarrow M(x, y, z). \quad (6)$$

This mapping is achieved in two steps with the use of the wavefield P : 1. The first step, the downward continuation, is to derive the wavefield at any depth $P(x_g, y_g, z | x_s, y_s, z; t)$ from the wavefield at the surface $P(x_g, y_g, 0 | x_s, y_s, 0; t)$. The downward continuation is possible because P is an up-going solution to the scalar wave equation, hence providing all the necessary information for the extrapolation. 2. The second step, the imaging, is to restrict $P(x_g, y_g, z | x_s, y_s, z; t)$ by applying the so called imaging condition $t = 0$ and hence obtaining a quantity which is a function of reflectivity, i.e. $P(x_g, y_g, z | x_s, y_s, z; 0)$. The goal of this second step is to pinpoint the exact moment when the wave "turns", i.e. transforms from a down-going into an up-going wave due to the interaction with the reflector. The two steps, and hence the entire migration concept, can be expressed as

$$M(x, y, z) = F [P(x, y, z | x, y, z; 0)], \quad (7)$$

i.e. the reflectivity M is a function F of the extrapolated data P at time $t = 0$. The simplest choice of F is the unit operator although this is not the preferred choice (see Stolt and Benson Ch 3).

When the velocity is constant, the wavefield at the measurement surface (the data) can be decomposed into plane-wave components and the extrapolation at any depth z can be

obtained simply by applying a phase-shift $e^{ik_z z}$, on both source and receiver, to each component, where k_z is the vertical wave-number of the plane-wave component being downward continued. To express this notion in mathematics, we first decompose P to planewaves using a Fourier Transform written as

$$P(k_{gx}, k_{gy}, 0 | k_{sx}, k_{sy}, 0; \omega) = \int dx_g \int dy_g \int dx_s \int dy_s \int dt e^{i(\omega t - k_{gx}x_g - k_{gy}y_g + k_{sx}x_s + k_{sy}y_s)} P(x_g, y_g, 0 | x_s, y_s, 0; t), \quad (8)$$

where $k_{gx}^2 + k_{gy}^2 + k_{gz}^2 = \omega^2/c_0^2$ and $k_{sx}^2 + k_{sy}^2 + k_{sz}^2 = \omega^2/c_0^2$ with c_0 the wave speed in the reference medium. This dispersion relation fixes k_{gz} and k_{sz} once the other parameters are chosen so that

$$k_{gz} = -\text{sgn}(\omega) \sqrt{\frac{\omega^2}{c_0^2} - k_{gx}^2 - k_{gy}^2} \quad (9)$$

and

$$k_{sz} = -\text{sgn}(\omega) \sqrt{\frac{\omega^2}{c_0^2} - k_{sx}^2 - k_{sy}^2}. \quad (10)$$

Notice that both wavenumbers have the same sign even though the extrapolation of source coordinates carries different sign than the extrapolation of receiver coordinates. This happens however because, for reflection data, we have a down-going wave on the source side and an up-going wave on the receiver side which changes the signs again hence canceling the previous effect.

The downward continuation of both source and receiver at a common depth z takes the form

$$P(k_{gx}, k_{gy}, z | k_{sx}, k_{sy}, z; \omega) = P(k_{gx}, k_{gy}, 0 | k_{sx}, k_{sy}, 0; \omega) e^{i(k_{gz} + k_{sz})z} \quad (11)$$

with k_{gz} and k_{sz} given by equations (9) and (10). To obtain P in the space domain we have to take the inverse Fourier Transform

$$P(x_g, y_g, z | x_s, y_s, z; t) = \frac{1}{(2\pi)^5} \int dk_{gx} \int dk_{gy} \int dk_{sx} \int dk_{sy} \int d\omega e^{i(-\omega t + k_{gx}x_g + k_{gy}y_g - k_{sx}x_s - k_{sy}y_s)} P(k_{gx}, k_{gy}, z | k_{sx}, k_{sy}, z; \omega), \quad (12)$$

and by setting $t = 0$ in the above equation we obtain

$$P(x_g, y_g, z | x_s, y_s, z; 0) = \frac{1}{(2\pi)^5} \int dk_{gx} \int dk_{gy} \int dk_{sx} \int dk_{sy} \int d\omega e^{i(k_{gx}x_g + k_{gy}y_g - k_{sx}x_s - k_{sy}y_s)} P(k_{gx}, k_{gy}, z | k_{sx}, k_{sy}, z; \omega). \quad (13)$$

The implementation of equation (13) is called phase-shift migration.

5 A comparison between travel time t and intercept time τ

The imaging concept in the migration procedure described in Section 4, assumes that the turning point of the wavefield is a point in space and hence, by restricting the time t to zero, we would obtain the location where an up-going wave would co-exist with the first arrival of a down-going wave, hence the position in space of the reflector. While this is true for regular reflections, it is not true for events which contain horizontal parts in their propagation paths. As Figure 1 shows, the turning point of a headwave is not a point in space but an entire linear horizontal propagation. In consequence, an imaging condition $t = 0$ on the data which contains these kind of events would interpret them as regular reflections and hence it would "create" reflectors at wrong depths to accommodate them. In this section we describe the connection and differences between the travel time t and the intercept time τ and show that the imaging condition $\tau = 0$ is a generalization of $t = 0$ which would image the headwaves from horizontal interfaces at the correct depth.

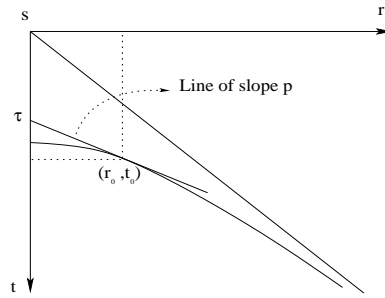


Figure 5: *The definition of the vertical time τ .*

By definition, the intercept or vertical time τ of an event arriving at offset r_0 in travel-time t_0 is the vertical component of the travel-time t_0 or, in other words, t_0 projected to zero offset along a line of slope p through the point (r_0, t_0) . (see Figure 5). The slope p of the tangent to the curve representing a reflection in the shot record pictured can be calculated as

$$p = \left(\frac{dt}{dr} \right)_{(r_0, t_0)} \quad (14)$$

and hence it represent the horizontal slowness associated with that particular arrival. The equation of the tangent line gives a relationship between the travel-time t and the vertical time τ of a particular arrival

$$t = \tau + pr. \quad (15)$$

This formula represents a decomposition of the total time into a horizontal time, pr , and a vertical time τ . To better understand this decomposition, consider a plane-wave component of constant horizontal slowness p of a wavefield produced by a 3D point source and moving through a medium with constant velocity c_0 . The points of intersections of this planewave

with the horizontal interface and the vertical line, move along them with constant respective speeds c_H and c_V such that

$$\sin i = \frac{c_0}{c_H} \quad (16)$$

and

$$\cos i = \frac{c_0}{c_V} \quad (17)$$

(see Figure 6a). The horizontal and the vertical slowness, p and q , are defined as

$$p = \frac{1}{c_H} = \frac{\sin i}{c_0} \quad (18)$$

and

$$q = \frac{1}{c_V} = \frac{\cos i}{c_0} \quad (19)$$

and they are related through

$$p^2 + q^2 = \frac{1}{c_0^2}. \quad (20)$$

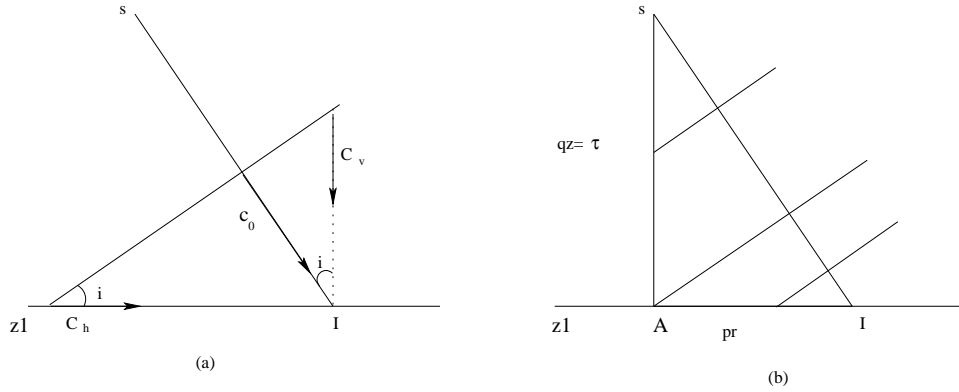


Figure 6: *The relationship between t and τ .*

Notice (from Figure 6b) that for the plane-wave to go from the source s to the incidence point I in time t is equivalent for the projection point onto the vertical to go from s to A along the vertical with the speed c_V and for the projection point onto the horizontal to go from A to I along the interface with the speed c_H . In this way the total time t is decomposed into two parts, a vertical and a horizontal time corresponding to the horizontal and vertical motion of the projection points as follows

$$t = \frac{z_1}{c_V} + \frac{r}{c_H} = qz_1 + pr = \tau + pr. \quad (21)$$

From the previous equation (21), the condition $t = 0$ always implies $\tau = 0$. The converse is not true. For a regular reflection $\tau = 0$ does imply that $t = 0$. To show this notice that $\tau = 0$ implies that no vertical propagation takes place, hence $z_1 = 0$. However for this type

of event there is a relationship between the horizontal and the vertical coordinates, r and z , namely

$$z \tan i = r \quad (22)$$

and so $z_1 = 0$ implies $r = 0$ and they both imply $t = 0$ (from equation (21)).

The same statement (and argument to prove it) applies to other events for which there is a similar relationship between the horizontal and the vertical coordinates (for example for a turning wave). However this is not true for all seismic events. For events that contain horizontal parts in their propagation paths, for example a headwave from a horizontal interface, there is no relationship between r and z ; in fact, for the part where the ray travels horizontally, we have $z = 0$ (no vertical propagation) while $r \neq 0$. In this case it is obvious that $\tau = 0$ does not imply $t = 0$.

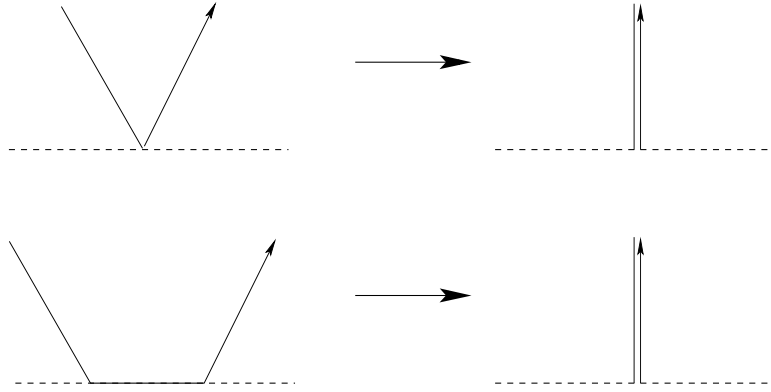


Figure 7: Events in t and τ : the left column shows a reflection and a headwave in travelttime t ; the right column is showing the same events in the vertical time τ .

The result we want to emphasize is that

$$\begin{aligned} t = 0 &\Rightarrow \tau = 0 \\ \tau = 0 &\not\Rightarrow t = 0 \end{aligned} \quad (23)$$

which implies that the imaging condition $\tau = 0$ is more general than $t = 0$. To image with $\tau = 0$ means to consider only the up-down motion of the wave and disregard any horizontal displacement that it might have (see Figure 7). This way, headwaves from horizontal interfaces are regarded as a down-up motion, rather than the down-lateral-up, and the imaging condition seeks the point where the wave turns, i.e. it changes from a downward into an upward propagation.

6 Analytic example

In this section we describe an analytic example of imaging headwaves with constant velocity phase-shift migration but with $\tau = 0$ imaging condition instead of $t = 0$. The purpose of

the example is to show, as stated before, that the both headwaves from horizontal interfaces and reflections are imaged at the correct depth with $\tau = 0$.

We consider a 3D acoustic experiment with source and receiver located at the same depth ($z = 0$) and one horizontal interface located at depth z_1 separating two media with wave propagation velocities c_0 and c_1 . The media are assumed to have no lateral variation. The post-critical data in such an experiment is (see e.g. Aki and Richards Ch. 6)

$$P(x_g, y_g, 0 | x_s, y_s, 0; \omega) = P^R(x_g, y_g, 0 | x_s, y_s, 0; \omega) + P^H(x_g, y_g, 0 | x_s, y_s, 0; \omega) \quad (24)$$

where

$$P^R(x_g, y_g, 0 | x_s, y_s, 0; \omega) = \frac{R}{d} \exp(ik_r r + i\nu_0 2z_1) \quad (25)$$

is the reflected event and

$$P^H(x_g, y_g, 0 | x_s, y_s, 0; \omega) = \frac{i}{\omega} \frac{c_0^2}{(1 - c_0^2/c_1^2)} \frac{1}{r^{1/2} L^{3/2}} \exp\left(i\omega \frac{r}{c_1} + i\nu_0 2z_1\right) \quad (26)$$

is the headwave. In these expressions $(x_s, y_s, 0)$ and $(x_g, y_g, 0)$ are the positions of the source and receiver respectively, ω is the temporal frequency, R is the angle-dependent reflection coefficient, d is the total distance from the source to reflection point to receiver, r is the horizontal offset and satisfies $r = \sqrt{(x_g - x_s)^2 + (y_g - y_s)^2}$, k_r is its conjugate in the K-space domain, ν_0 is the vertical wavenumber of the first medium and satisfies $\nu_0^2 + k_r^2 = \omega^2/c_0^2$, and L is the length of the horizontal part of the ray representation of the headwave.

We downward continue both the source and receiver to same arbitrary depth and obtain

$$P(x_g, y_g, z | x_s, y_s, z; \omega) = P^R(x_g, y_g, z | x_s, y_s, z; \omega) + P^H(x_g, y_g, z | x_s, y_s, z; \omega) \quad (27)$$

where

$$P^R(x_g, y_g, z | x_s, y_s, z; \omega) = \frac{R}{d} \exp(ik_r r + i\nu_0 2(z_1 - z)) \quad (28)$$

and

$$P^H(x_g, y_g, z | x_s, y_s, z; \omega) = \frac{i}{\omega} \frac{c_0^2}{(1 - c_0^2/c_1^2)} \frac{1}{r^{1/2} L^{3/2}} \exp\left(i\omega \frac{r}{c_1} + i\nu_0 2(z_1 - z)\right). \quad (29)$$

The reflection can be easily imaged with the $t = 0$ imaging condition to obtain the reflectivity of the reflection point at the correct depth z_1 . The same procedure, applied to the part of the data representing the headwave, would assume that the turning point of that event is a point in space and it would seek that point hence creating an image at the wrong depth.

To image the headwave with $\tau = 0$ we first inverse Fourier Transform to bring the data back to the time domain. However, ω is conjugated to the travel time t and we want to bring the data back to the vertical time τ domain where we can apply the imaging condition. We define the image I to be

$$I(\tau) = \int d\Omega e^{-i\Omega\tau} P^H(x_g, y_g, z | x_s, y_s, z; \omega) \quad (30)$$

where

$$\Omega = \omega \left(1 + \frac{r}{c_1 \tau} \right). \quad (31)$$

With the full expression for P^H we have

$$I(\tau) = \int d\Omega e^{-i\Omega\tau} A(\omega) \exp \left(i\omega \frac{r}{c_1} + i\nu_0 2(z_1 - z) \right) \quad (32)$$

where $A(\omega)$ is the amplitude in equation (29). By plugging in the expression (31) for Ω we obtain

$$I(\tau) = \int d\Omega e^{-i\omega\tau} A(\omega) \exp (i\nu_0 2(z_1 - z)) \quad (33)$$

and after imaging with $\tau = 0$ we find

$$I(\tau = 0) = \int d\Omega A(\omega) \exp (i\nu_0 2(z_1 - z)). \quad (34)$$

This last expression represents a delta like event at the correct depth z_1 hence showing that the headwave is imaged correctly.

Notice that the new condition discards any horizontal propagation (and time associated with it) and only takes into consideration down-up propagations, as one can also see from Figure 7. For the headwave this means discarding the horizontal propagation along the interface. It is not difficult to see that the procedure outlined above also images the reflection data at the correct depth.

7 Conclusions

The purpose of this paper is to present the advantages of imaging with $\tau = 0$ versus imaging with $t = 0$. The former condition is a generalization of the latter which has the ability to image headwaves from horizontal interfaces at the correct depth. This suggests that using $\tau = 0$ in the internal multiples attenuation algorithm derived from inverse scattering series techniques would generalize it to address internal multiples constructed with this kind of sub-events. This research is part of our strategy to include more of the returning signal, information bearing or not, in our analysis and processing.

References

- Aki and Richards (1980) *Quantitative Seismology*, v1, W.H Freeman and Company, San Francisco.
- Clayton R. W., McMechan G. A. (1981) Inversion of refraction data by wavefield continuation, *Geophysics*, **46**, pp. 860-868.

- Cerveny and Ravindra (1971) Theory of seismic headwaves, University of Toronto Press.
- Dragoset W. (2003) Multiples Forum, University of Houston.
- Gazdag, J. (1978) Wave equation migration with the phase-shift method, *Geophysics*, **43**, pp. 1342-1351.
- Gel'fand I.M., Graev M.I., Vilenkin N.Y. (1966) Generalized functions, v. 5, Integral geometry and representation theory, New York Academic Press.
- Jeffreys, H. (1926) On compressional waves in two superposed layers, *Proceedings of the Cambridge Philosophical Society* **23**, pp. 472-481.
- Lowenthal R., Roverson L., Lu R, Sherwood J. (1976) The wave equation applied to migration, *Geophysical Prospecting*, **24**, pp. 380-399.
- Stolt R. H. and Benson A. K. (1986) Seismic Migration, Theory and Practice, v 5, Geophysical Press Limited.
- Weglein A. B., Araujo F.V., Carvalho P. M., Stolt R. H., Matson K. H., Coates R., Corrigan D., Foster D. J., Shaw S. A., Zhang H. *Inverse scattering series and seismic exploration*, Topical Review Inverse Problems, 19, pp. R27-R83.